

# Pressure-Induced Valence Change and Semiconductor–Metal Transition in $\text{PbCrO}_3$

Min Wu,<sup>†</sup> Lirong Zheng,<sup>†</sup> Shengqi Chu,<sup>†</sup> Zhenxing Qin,<sup>‡,§</sup> Xiao-Jia Chen,<sup>||,‡</sup> Chuanlong Lin,<sup>†</sup> Zheng Tang,<sup>†</sup> and Tiandou Hu<sup>\*,†,⊥</sup>

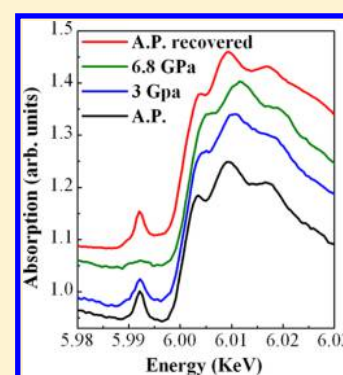
<sup>†</sup>Beijing Synchrotron Radiation Facility, Institute of High Energy Physics, Chinese Academy of Sciences, Beijing 100049, China

<sup>‡</sup>Department of Physics, South China University of Technology, Guangzhou 510640, China

<sup>§</sup>School of Applied Science, Taiyuan University of Science and Technology, Taiyuan 030024, China

<sup>||</sup>Center for High Pressure Science and Technology Advanced Research, Shanghai 201203, China

**ABSTRACT:** Pressure-induced valence change and semiconductor–metal transition were revealed in perovskite compound  $\text{PbCrO}_3$  by X-ray absorption spectroscopy (XAS) and resistance measurements, respectively. The Cr  $L_{2,3}$  edge XAS spectra indicate a charge disproportionation of Cr ( $3\text{Cr}^{4+} \rightarrow 2\text{Cr}^{3+} + \text{Cr}^{6+}$ ) at ambient pressure, suggesting that the ambient-pressure phase of  $\text{PbCrO}_3$  has complex local structure and cannot be explained using the simple cubic perovskite structure ( $Pm\text{-}3m$ ). Upon compression up to 4.2 GPa,  $\text{Cr}^{3+}$  and  $\text{Cr}^{6+}$  ions were converted to  $\text{Cr}^{4+}$  via charge transfer, associated with semiconductor–metal transition. The high-pressure metal phase is determined to be cubic perovskite structure ( $Pm\text{-}3m$ ). Compared with the previous X-ray diffraction experiment, the large volume collapse ( $\sim 9.8\%$  at 1.6 GPa) may be related to valence change and semiconductor–metal transition.



## INTRODUCTION

The chromate perovskites  $\text{RCrO}_3$  ( $R = \text{Sr}, \text{Ca}$ ), which present the  $\text{Cr}^{4+}$  ion in octahedral coordinations, have been much studied due to their anomalous electronic and magnetic states for the past few years.<sup>1–5</sup>  $\text{PbCrO}_3$  was first synthesized at high pressures and high temperatures in the late 1960s.<sup>6,7</sup> Previous X-ray and neutron diffraction experiments showed that  $\text{PbCrO}_3$  has a cubic perovskite structure with anomalously large volume.<sup>6–8</sup> Its lattice parameter (4.00 Å) is much larger than cubic  $\text{SrCrO}_3$  (3.82 Å) even though the atomic radius of Sr (1.44 Å) is similar to that of Pb (1.49 Å).<sup>1</sup>  $\text{PbCrO}_3$  was considered as a perovskite compound with the  $\text{Cr}^{4+}$  ion occupying the octahedral site, coordinated with six oxygen atoms.<sup>6,7,9</sup> However, recent electron diffraction and high-resolution microscopy study revealed that the microstructure of  $\text{PbCrO}_3$  is a rather complex perovskite with superlattice structure of  $a_p \times 3a_p \times (14\text{--}18)a_p$ , where  $a_p$  is the lattice constant of the cubic perovskite structure.<sup>10</sup> On the other hand, Ganesh et al. suggested a tetragonal structure which is more stable than cubic perovskite structure at ambient pressure for  $\text{PbCrO}_3$  from density functional theory (DFT)+ $U$  calculations.<sup>11</sup> In the first-principle local density approximation (LDA)+ $U$ , Wang et al. indicated a mixture of  $\text{PbCrO}_3\text{--CrPbO}_3$  at ambient pressure.<sup>12</sup> In the mixture model of  $\text{PbCrO}_3\text{--CrPbO}_3$ ,  $\text{CrO}_6$  in  $\text{CrPbO}_3$  is converted to  $\text{PbO}_6$ . Cr ions occupy two different sites in the structure. Theoretical calculation shows that the cubic perovskite structure  $\text{PbCrO}_3$  should be a conductor,<sup>13,14</sup> whereas experimental results demonstrated that  $\text{PbCrO}_3$  is a semiconductor.<sup>8,15,16</sup> Therefore,

the structure of  $\text{PbCrO}_3$  at ambient conditions is still controversial. Here, we report a charge disproportionation phenomenon in  $\text{PbCrO}_3$  and bring a new way for understanding this issue.

Recently, it was surprisingly found by Xiao et al. that  $\text{PbCrO}_3$  underwent an isostructural phase transition with large volume collapse of approximate 9.8% at 1.6 GPa. This is one of the largest volume collapses known for transition-metal oxides.<sup>17</sup> The isostructural phase transitions induced by high pressures were usually considered to be originating from the electronic structural change.<sup>18–20</sup> However, they considered the high-pressure phase transition of  $\text{PbCrO}_3$  not to be related with any change of electronic state but could be related to the abnormally large volume and compressibility. In contrast, Ganesh et al. attributed the large volume collapse to the first-order transition from a tetragonal structure to a cubic phase in the density functional theory (DFT)+ $U$  calculation,<sup>11</sup> whereas Wang et al. indicated that the large volume change stems from the R3 phase of  $\text{PbCrO}_3\text{--CrPbO}_3$  to the cubic perovskite  $\text{PbCrO}_3$  transition which is accompanied by an insulator–metal transition.<sup>12</sup> In these studies, the structure of the ambient-pressure (AP) phase remains controversial, while theoretical and experimental results supported that the high-pressure (HP) phase has the cubic perovskite structure. Experiments, especially the X-ray absorption spectroscopy (XAS) and

Received: July 20, 2014

Revised: August 31, 2014

Published: September 11, 2014

resistance measurements which can provide information on valence change and electron transport, are required to study the local structure of the AP phase, relationship of the AP and HP phases, and mechanism of large volume collapse in the phase transition.

In this paper we investigate the change of the electronic state of  $\text{PbCrO}_3$  at different pressures by XAS. Additionally, resistance measurements were performed to investigate the change of the electron transport property at high pressure. A pressure-induced valence change and a pressure-induced semiconductor–metal transition were observed. We analyzed the unusual properties of AP phase  $\text{PbCrO}_3$  and attributed the large volume collapse of phase transition to the charge transfer between chromium ions associated with semiconductor–metal transition.

## EXPERIMENTAL SECTION

The  $\text{PbCrO}_3$  samples were synthesized from high purity yellow  $\text{PbO}$  and black  $\text{CrO}_2$  powder with a cubic anvil-type high-pressure apparatus. The mixture was treated at 5.8 GPa and 1200 °C for 30 min and quenched to room temperature prior to the release of pressure. Powder X-ray diffraction experiments ( $\lambda = 0.6199 \text{ \AA}$ ) for sample identification were carried out in the 4W2 beamline at Beijing Synchrotron Radiation Facility (BSRF), China. The XRD results are consistent with the cubic perovskite structure and space group  $Pm\bar{3}m$ , and the lattice constant ( $a = 4.005 \text{ \AA}$ ) is in accordance with previous reports.<sup>6–8,16,17</sup> A small number of weak peaks from impurities can also be seen (Figure 1). The Cr  $L_{2,3}$  edge XAS

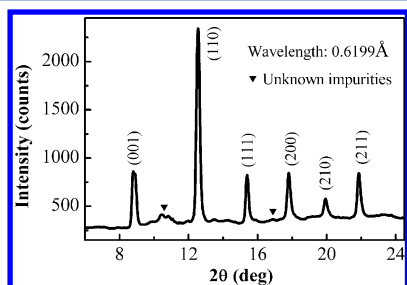


**Figure 1.** Powder X-ray diffraction pattern of the  $\text{PbCrO}_3$  sample used for our experiments. These diffraction experiments ( $\lambda = 0.6199 \text{ \AA}$ ) were carried out in the 4W2 beamline at Beijing Synchrotron Radiation Facility (BSRF), China.

measurements were performed in total electron yield (TEY) mode at the beamline 4B9B of BSRF. The  $\text{PbCrO}_3$  and reference samples were measured under an ultrahigh vacuum of  $\sim 10^{-10}$  Torr at room temperature. The XAS measurements at the Cr K edge under various pressures were carried out at the beamline 1W1B of BSRF. The diamond anvil cell (DAC) with a pair of perforated diamond anvils<sup>21</sup> was used to lessen the absorption of diamond and apply the pressure up to 7.6 GPa. The powdered sample and amorphous B powder as a pressure medium were mixed and steered inside the DAC. A polycapillary X-ray optic was used to focus the X-ray and reduce the disturbance from the diffraction and absorption of diamond.<sup>22</sup> The high-pressure experiments for resistance measurement were carried out using DAC with culets of 500  $\mu\text{m}$ . A small piece of impacted  $\text{PbCrO}_3$  powder was loaded into the sample hole of  $\sim 100 \mu\text{m}$  in the stainless steel gasket. Four electrodes were attached to the sample and insulated from the gasket. No extra pressure medium was used. The pressures in

all experiments were determined by measuring the wavelength of ruby fluorescence<sup>23</sup> and measured at room temperature.

## RESULTS AND DISCUSSION

The 3d transition-metal  $L_{2,3}$  absorption edges are from the  $2p \rightarrow 3d$  transition and sensitive to the valence state.<sup>24</sup> The chemical shift (about 0.7 eV toward higher energy for one valence increase) between the different Cr oxidation states is clearly visible at the  $L_{2,3}$  edges.<sup>25</sup> Figure 2(a) shows the Cr  $L_{2,3}$

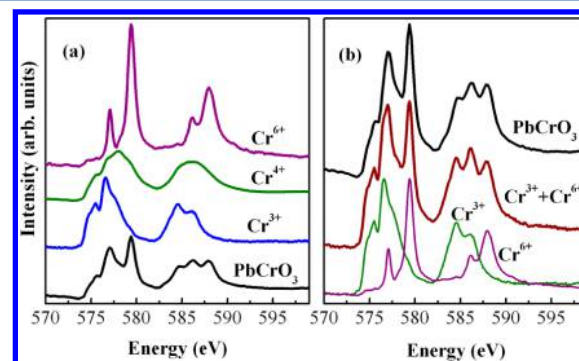


**Figure 2.** (a) Cr  $L_{2,3}$  edge XAS spectra for  $\text{PbCrO}_3$  and reference samples ( $\text{PbCrO}_4$ ,  $\text{CrO}_2$ ,  $\text{Cr}_2\text{O}_3$ ). (b) Spectra of  $\text{PbCrO}_3$  compared to the weighted sum of spectra of  $\text{Cr}^{3+}$  and  $\text{Cr}^{6+}$ .

edge XAS spectra of AP phase  $\text{PbCrO}_3$  (under ultrahigh vacuum actually) and reference samples ( $\text{PbCrO}_4$ ,  $\text{CrO}_2$ ,  $\text{Cr}_2\text{O}_3$ ). The peaks centered at 575.6 and 579.4 eV in the  $L_3$  edge of  $\text{PbCrO}_3$  are aligned with the  $\text{Cr}^{3+}$  ( $\text{Cr}_2\text{O}_3$ ) and  $\text{Cr}^{6+}$  ( $\text{PbCrO}_4$ ) reference samples, respectively, and the same as the peaks centered at 584.6 and 588 eV in the  $L_2$  edge. The absence of  $\text{Cr}^{4+}$  peaks and the “0.7 eV principle” reveal that the Cr ions maybe are  $\text{Cr}^{3+}$  and  $\text{Cr}^{6+}$ , rather than  $\text{Cr}^{4+}$ . The weighted sum of spectra of  $\text{Cr}^{3+}$  and  $\text{Cr}^{6+}$ , in a ratio of two to one, agrees with the experimental spectra of  $\text{PbCrO}_3$  well [Figure 2(b)]. This shows that the Cr ions dissociate into  $\text{Cr}^{3+}$  and  $\text{Cr}^{6+}$  via charge transfer in AP phase  $\text{PbCrO}_3$  ( $\text{Pb}^{2+}\text{Cr}^{3+}_{2/3}\text{Cr}^{6+}_{1/3}\text{O}_3$ ), and AP phase  $\text{PbCrO}_3$  has a complex structure which cannot be described by a simple cubic perovskite structure.

The valence dissociation is also supported by the bond valence model which can provide information on the valence state of the AP and HP phase  $\text{PbCrO}_3$ . The bond valence sum (BVS) relates the metal valence  $V$  to the metal oxygen distance  $r_i$ .<sup>26</sup> For each central atom

$$V = \sum s_i, \quad s_i = \exp[(r_0 - r_i)/B]$$

where  $B$  is a constant of  $0.37 \text{ \AA}$  and  $r_0$  is the standard parameter for  $\text{Sr}^{2+}$ ,  $\text{Ca}^{2+}$ ,  $\text{Pb}^{2+}$ , and  $\text{Cr}^{4+}$ .<sup>26,27</sup> Table 1 shows the calculation results for  $\text{SrCrO}_3$ ,  $\text{CaCrO}_3$ , and AP and HP phase  $\text{PbCrO}_3$ . The structure information on  $\text{SrCrO}_3$ ,  $\text{CaCrO}_3$ , and HP phase  $\text{PbCrO}_3$  is from previous research papers.<sup>1,17</sup> The BVSs for the

**Table 1.** Bond Valence Sums<sup>a</sup> for  $\text{SrCrO}_3$ ,  $\text{CaCrO}_3$ , AP Phase  $\text{PbCrO}_3$ , and HP Phase  $\text{PbCrO}_3$

$\text{SrCrO}_3$		$\text{CaCrO}_3$		AP phase		HP phase	
Cr	Sr	Cr	Ca	Cr	Pb	Cr	Pb
4.14	2.48	4.19	2.32	3.25	1.73	4.01	2.33

<sup>a</sup> $V = \sum s_i, s_i = \exp[(r_0 - r_i)/B]$ . Values calculated using  $r_0 = 2.118$  for  $\text{Sr}^{2+}$ , 1.967 for  $\text{Ca}^{2+}$ , 2.112 for  $\text{Pb}^{2+}$ , and 1.773 for  $\text{Cr}^{4+}$ .

HP phase are similar to that for the  $\text{Cr}^{4+}$  perovskites  $\text{SrCrO}_3$  and  $\text{CaCrO}_3$ , which confirm that the HP phase is  $\text{Pb}^{2+}\text{Cr}^{4+}\text{O}_3$ . In contrast, the BVSs for the AP phase are significantly smaller as the bond distance is enhanced. This deviation implies that the simple cubic structure with  $\text{Cr}^{4+}$  cannot describe the AP phase exactly, which agrees with the XAS spectra. The two different Cr sites model of  $\text{PbCrO}_3\text{--CrPbO}_3$  has been suggested for the AP phase;<sup>12,17</sup> however, the details of local structure in AP phase  $\text{PbCrO}_3$  are still ambiguous, and more study is needed.

Since Cr atoms may have different valence states in the AP and HP phase, pressure-induced valence change could be directly observed during compression. To identify the valence change of Cr induced by pressure, XAS experiments on the Cr K absorption edge were carried out. Figure 3 shows the Cr K

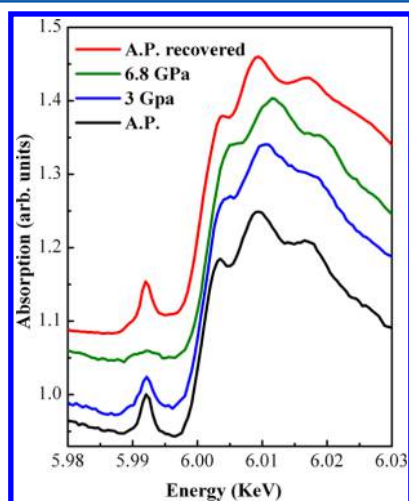


**Figure 3.** Cr K edge XAS spectra for  $\text{PbCrO}_3$  at various pressures. The pressure-induced shift of the absorption edge energy and the disappearance of the pre-edge peak can be observed.

edge XAS spectra of  $\text{PbCrO}_3$  collected at room temperature and different pressures. There are two obvious differences between the AP and HP (6.8 GPa) phases: the pressure-induced shift of the absorption edge energy ( $E_0$ ) and the disappearance of the pre-edge peak.  $E_0$  is a good measure of the Cr valence change.  $E_0$  of the Cr K edge has been reported to be linearly dependent on the Cr valence.<sup>28</sup> The pressure-induced valence change is indicated by the shift of the pressure dependence of  $E_0$  in Figure 4, which was determined from the maximum position of the first derivative of the observed XAS

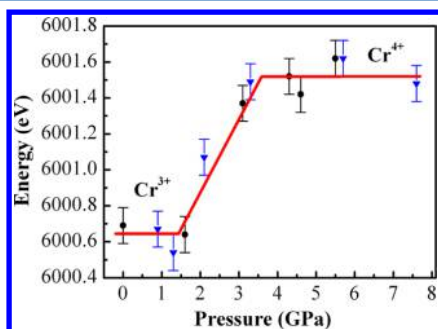


**Figure 4.** Pressure dependence of absorption edge energy around Cr K XAS spectra for  $\text{PbCrO}_3$ . The circle and triangle indicate separate experiments. The lines are guides to the eyes.

spectra. The detected about  $0.8 \pm 0.2$  eV  $E_0$  shift from the AP phase to the HP phase indicates the increase in Cr valence together with structural phase transition. As mentioned above, all the previous studies support the cubic perovskite structure for HP phase  $\text{PbCrO}_3$  where Cr ions are tetravalent. This means that the application of pressure leads to the transition of  $\text{Cr}^{3+}$  to  $\text{Cr}^{4+}$  by charge transfer. Additionally, the  $\text{Cr}^{6+}$  ions should also change to  $\text{Cr}^{4+}$  during compression since the AP phase includes  $\text{Cr}^{3+}$  and  $\text{Cr}^{6+}$  ions indicated by the Cr  $L_{2,3}$  edge spectra. The pre-edge peak has been assigned as the  $1s \rightarrow 3d$  transition. This transition is strictly dipole forbidden in the HP phase which contains regular octahedral  $\text{CrO}_6$  units, and the strong pre-edge peak at ambient pressure indicates that the symmetry of the ligands is lowered.<sup>29</sup> The pre-edge peak for  $\text{Cr}^{3+}$  with six oxygen coordinations is quite weak, so the strong feature can be considered as the fingerprint of  $\text{Cr}^{6+}$ . Upon compression, the pre-edge peak decreases in relative intensity and almost disappears at 6.8 GPa, indicating the valence change of  $\text{Cr}^{6+}$  to  $\text{Cr}^{4+}$ .

The valence change could be associated with the change of the electron transport properties. Therefore, we further performed the resistance measurement at pressures, as shown in Figure 5. Resistance at room temperature has a steep drop by

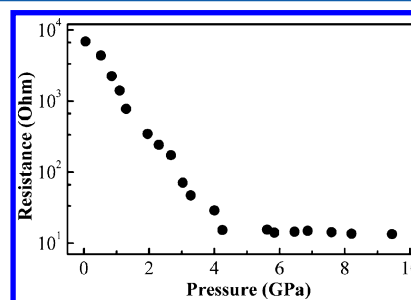


**Figure 5.** Pressure dependence of resistance of  $\text{PbCrO}_3$  at room temperature. Resistance has a steep drop by 3 orders of magnitude.

3 orders of magnitude in the pressure range of AP to 4.2 GPa. Above 4.2 GPa the resistance of the HP phase changes trivially. The data of temperature-dependent resistance collected at ambient pressure and 8.2 GPa (HP) are also shown in Figure 6. As theory calculations have predicted,<sup>11,12</sup> metallic conductivity of the HP phase  $\text{PbCrO}_3$  is clearly visible in Figure 6(a). However, then the AP phase  $\text{PbCrO}_3$  exhibits a semiconducting behavior in the temperature range between 195 and 300 K (see Figure 6(b)), which agrees with the results previously reported.<sup>8,15,16</sup> As plotted in the inset of Figure 6(b), the resistance in this range can be described by the activation law

$$R = R_0 \exp[\Delta/(2k_B T)]$$

with different activation energy  $\Delta_1 \sim 0.47$  eV and  $\Delta_2 \sim 0.24$  eV.  $R_0$  is constant, and  $k_B$  is the Boltzmann constant. This abnormal change of activation energy at temperature around 213 K was also observed by Arévalo-López et al. with different values (0.11–0.26 eV at 245 K).<sup>15</sup> The results of activation energy, 0.27 and 0.5 eV, were also reported by different researchers.<sup>8,16</sup> These can unambiguously prove that the  $\text{PbCrO}_3$  causes a pressure-induced semiconductor–metal transition,<sup>30</sup> in agreement with Wang's theoretical calculation.<sup>12</sup> Recently a high-pressure resistance experiment of  $\text{PbCrO}_3$  was performed in a cubic press apparatus up to 4.1 GPa.<sup>31</sup> The same steep drop of resistance at room temperature was

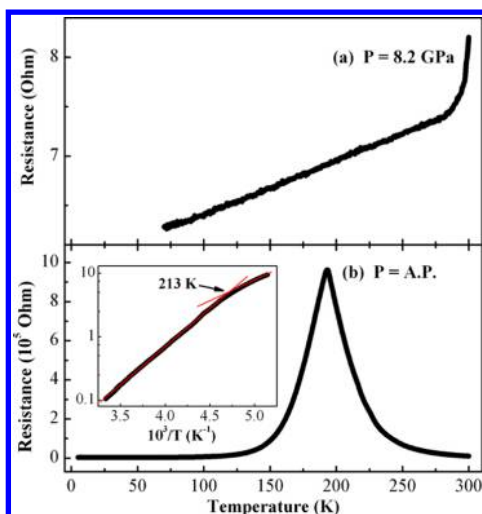


**Figure 6.** Temperature dependence of resistance of (a) high-pressure phase (8.2 GPa) and (b) ambient-pressure phase  $\text{PbCrO}_3$ . Inset: Arrhenius plot of AP phase  $\text{PbCrO}_3$ , from 300 to 195 K, indicates two activation energies with 0.47 and 0.24 eV.

observed; however, a semiconducting behavior showed at 4.1 GPa at high temperature. Considering the different measured pressure and temperature ranges, this result may also represent the electrical nature of the HP phase  $\text{PbCrO}_3$ . It is noteworthy that below 195 K the AP phase  $\text{PbCrO}_3$  shows a metallic trend [Figure 6(b)], and it is possible that the HP phase has a similar behavior at high temperature. More studies about this electrical transport are needed.

The valence change should also exist during the releasing sample since  $\text{PbCrO}_3$  is synthesized via  $\text{PbO} + \text{CrO}_2 \rightarrow \text{PbCrO}_3$  at 5.8 GPa. The compound with  $\text{Cr}^{4+}$  is rare as  $\text{Cr}^{4+}$  is relatively unstable.<sup>32</sup> High pressure is a necessary condition to preserve  $\text{Cr}^{4+}$  and stabilize  $\text{PbCrO}_3$  at high temperature. Thus,  $\text{PbCrO}_3$  is a stable phase in the Pb–Cr–O system at high temperature and high pressure and decomposes into  $\text{Cr}_2\text{O}_3$  with  $\text{Cr}^{3+}$  and  $\text{Pb}_2\text{CrO}_5$  with  $\text{Cr}^{6+}$  when pressure decreases at high temperature.<sup>7</sup> We presume that high pressure (about 4.2 GPa) is still necessary to maintain the  $\text{Cr}^{4+}$  at room temperature. Then the Cr valence states dissociate as pressure reduces to ambient pressure, leading to the  $\text{CrO}_6$  octahedron distortion and abnormal large lattice constant. The previous XRD experiments performed by Xiao et al. showed the AP and HP phase have the same space group,<sup>17</sup> i.e., the same long-range structure, and the AP phase maybe is a metastable state during phase transition or decomposition of the HP phase. In perovskite-type 3d transition metal oxides like  $\text{RNiO}_3$ , the charge disproportionation was reported to induce the metal–insulator transition.<sup>33–36</sup> In this case, the occurrence of valence dissociation is most likely responsible for the phase transition and the charge localization in semiconducting AP phase  $\text{PbCrO}_3$ . If we substitute  $\text{Pb}^{2+}$  with smaller ions (such as  $\text{Sr}^{2+}$ ), the chemical pressure may suppress the valence dissociation, leading to a marked drop of lattice constant and resistivity ( $\text{SrCrO}_3$ ).<sup>1,16</sup>

## CONCLUSIONS

In summary, we report the valence change and semiconductor–metal transition in  $\text{PbCrO}_3$  for the first time. The high-pressure-synthesized cubic perovskites  $\text{PbCrO}_3$  with  $\text{Cr}^{4+}$  become unstable when the pressure is below 4.2 GPa.

Comparing the Cr  $L_{2,3}$  edge XAS spectra of  $\text{PbCrO}_3$  with a reference sample, we infer that the valence states of Cr ions dissociate into  $\text{Cr}^{3+}$  and  $\text{Cr}^{6+}$  at ambient pressure, and this valence change is supported by Cr K edge XAS under various pressures. In consequence charge change leads to a pressure-induced semiconductor–metal transition together with the phase transition. The ambient-pressure phase  $\text{PbCrO}_3$  has ambiguous local structure and maybe is just a metastable state, but more detailed research is needed.

## AUTHOR INFORMATION

### Corresponding Author

\*E-mail: hutd@ihp.ac.cn. Tel.: 86-10-8823 5980-1.

### Present Address

<sup>†</sup>19B Yuquan Lu, Shijingshan District, Institute of High Energy Physics, Chinese Academy of Sciences, Beijing, 100049, P. R. China.

### Notes

The authors declare no competing financial interest.

## ACKNOWLEDGMENTS

We thank Changqin Jin group for help synthesizing sample and Wansheng Xiao and Dayong Tan for useful discussions. This work was supported by the National Natural Science Foundation of China (Grant No. 11175202). The resistance measurements in SCUT were supported by the Cultivation Fund of the Key Scientific and Technical Innovation Project Ministry of Education of China (No.708070).

## REFERENCES

- Zhou, J. S.; Jin, C. Q.; Long, Y. W.; Yang, L. X.; Goodenough, J. B. Anomalous Electronic State in  $\text{CaCrO}_3$  and  $\text{SrCrO}_3$ . *Phys. Rev. Lett.* **2006**, *96*, 046408.
- Ortega-San-Martin, L.; Williams, A. J.; Rodgers, J.; Attfield, J. P.; Heymann, G.; Huppertz, H. Microstrain Sensitivity of Orbital and Electronic Phase Separation in  $\text{SrCrO}_3$ . *Phys. Rev. Lett.* **2007**, *99*, 255701.
- Komarek, A. C.; Streltsov, S. V.; Isobe, M.; Möller, T.; Hoelzel, M.; Senyshyn, A.; Trots, D.; Fernández-Díaz, M. T.; Hansen, T.; Gotou, H.; et al.  $\text{CaCrO}_3$ : An Anomalous Antiferromagnetic Metallic Oxide. *Phys. Rev. Lett.* **2008**, *101*, 167204.
- Streltsov, S. V.; Korotin, M. A.; Anisimov, V. I.; Khomskii, D. I. Band Versus Localized Electron Magnetism in  $\text{CaCrO}_3$ . *Phys. Rev. B* **2008**, *78*, 054425.
- Lee, K. W.; Pickett, W. E. Orbital-Ordering Driven Structural Distortion in Metallic  $\text{SrCrO}_3$ . *Phys. Rev. B* **2009**, *80*, 125133.
- Roth, W. L.; Devries, R. C. Crystal and Magnetic Structure of  $\text{PbCrO}_3$ . *J. Appl. Phys.* **1967**, *38*, 951–952.
- Devries, R. C.; Roth, W. L. High-Pressure Synthesis of  $\text{PbCrO}_3$ . *J. Am. Ceram. Soc.* **1968**, *51*, 72–75.
- Chamberland, B. L.; Moeller, C. W. A Study on the  $\text{PbCrO}_3$  Perovskite. *J. Solid State Chem.* **1972**, *5*, 39–41.
- Arevalo-Lopez, A. M.; Castillo-Martinez, E.; Alario-Franco, M. A. Electron Energy Loss Spectroscopy in  $\text{ACrO}_3$  (A = Ca, Sr and Pb) Perovskites. *J. Phys.: Condens. Matter* **2008**, *20*, 505207.
- Arévalo-López, Á. M.; Alario-Franco, M. Á. On the Structure and Microstructure of “ $\text{PbCrO}_3$ ”. *J. Solid State Chem.* **2007**, *180*, 3271–3279.
- Ganesh, P.; Cohen, R. E. Orbital Ordering, Ferroelasticity, and the Large Pressure-Induced Volume Collapse in  $\text{PbCrO}_3$ . *Phys. Rev. B* **2011**, *83*, 172102.
- Wang, B. T.; Yin, W.; Li, W. D.; Wang, F. W. First-Principles Study of Pressure-Induced Phase Transition and Electronic Property of  $\text{PbCrO}_3$ . *J. Appl. Phys.* **2012**, *111*, 013503.

- (13) Jaya, S. M.; Jagadish, R.; Rao, R. S.; Asokamani, R. Electronic Structure of the Perovskite Oxides SrCrO<sub>3</sub> and PbCrO<sub>3</sub>. *Mod. Phys. Lett. B* **1992**, *6*, 103–112.
- (14) Yıldırım, H.; Ağduk, S.; Gökoğlu, G. Electronic Structure of Antiferromagnetic PbCrO<sub>3</sub> (0 0 1) Surfaces. *J. Alloys Compd.* **2011**, *509*, 9284–9288.
- (15) Arévalo-López, Á. M.; Dos Santos-García, A. J.; Alario-Franco, M. Á. Antiferromagnetism and Spin Reorientation in “PbCrO<sub>3</sub>”. *Inorg. Chem.* **2009**, *48*, 5434–5438.
- (16) Komarek, A. C.; Möller, T.; Isobe, M.; Drees, Y.; Ulbrich, H.; Azuma, M.; Fernández-Díaz, M. T.; Senyshyn, A.; Hoelzel, M.; André, G.; et al. Magnetic Order, Transport and Infrared Optical Properties in the ACrO<sub>3</sub> System (A = Ca, Sr, and Pb). *Phys. Rev. B* **2011**, *84*, 125114.
- (17) Xiao, W. S.; Tan, D. Y.; Xiong, X. L.; Liu, J.; Xu, J. Large Volume Collapse Observed in the Phase Transition in Cubic PbCrO<sub>3</sub> Perovskite. *Proc. Natl. Acad. Sci. U.S.A.* **2010**, *107*, 14026–14029.
- (18) Maple, M. B.; Wohlbe, D. Nonmagnetic 4f Shell in the High-Pressure Phase of SmS. *Phys. Rev. Lett.* **1971**, *27*, 511–515.
- (19) Held, K.; McMahan, A. K.; Scalettar, R. T. Cerium Volume Collapse: Results from the Merger of Dynamical Mean-Field Theory and Local Density Approximation. *Phys. Rev. Lett.* **2001**, *87*, 276404.
- (20) Liu, B.; Han, Y. H.; Gao, C. X.; Ma, Y. Z.; Peng, G.; Wu, B. J.; Liu, C. L.; Wang, Y.; Hu, T. J.; Cui, X. Y.; et al. Pressure Induced Semiconductor-Semimetal Transition in WSe<sub>2</sub>. *J. Phys. Chem. C* **2010**, *114*, 14251–14254.
- (21) Soignard, E.; Benmore, C. J.; Yarger, J. L. A Perforated Diamond Anvil Cell for High-Energy X-ray Diffraction of Liquids and Amorphous Solids at High Pressure. *Rev. Sci. Instrum.* **2010**, *81*, 035110.
- (22) Li, Y. D.; Lin, X. Y.; Liu, S. G.; Zheng, L. R.; He, J. L.; Guo, F.; Sun, T. X. Application of a Polycapillary X-ray Optics in High Pressure XAFS. *J. Opt.* **2013**, *15*, 072601.
- (23) Mao, H. K.; Xu, J.; Bell, P. M. Calibration of the Ruby Pressure Gauge to 800-Kbar under Quasi-Hydrostatic Conditions. *J. Geophys. Res.* **1986**, *91*, 4673–4676.
- (24) de Groot, F. High-Resolution X-ray Emission and X-ray Absorption Spectroscopy. *Chem. Rev.* **2001**, *101*, 1779–1808.
- (25) Theil, C.; van Elp, J.; Folkmann, F. Ligand Field Parameters Obtained from and Chemical Shifts Observed at the Cr L<sub>2,3</sub> Edges. *Phys. Rev. B* **1999**, *59*, 7931–7936.
- (26) Brese, N. E.; O’keeffe, M. Bond-Valence Parameters for Solids. *Acta Crystallogr.* **1991**, *47*, 192–197.
- (27) Wood, R. M.; Abboud, K. A.; Palenik, R. C.; Palenik, G. J. Bond Valence Sums in Coordination Chemistry. Calculation of the Oxidation State of Chromium in Complexes Containing Only Cr-O Bonds and a Redetermination of the Crystal Structure of Potassium Tetra(peroxo)chromate(V). *Inorg. Chem.* **2000**, *39*, 2065–2068.
- (28) Pantelouris, A.; Modrow, H.; Pantelouris, M.; Hormes, J.; Reinen, D. The Influence of Coordination Geometry and Valency on the K-edge Absorption Near Edge Spectra of Selected Chromium Compounds. *Chem. Phys.* **2004**, *300*, 13–22.
- (29) Wong, J.; Lytle, F. W.; Messmer, R. P.; Maylotte, D. H. K-edge Absorption Spectra of Selected Vanadium Compounds. *Phys. Rev. B* **1984**, *30*, 5596–5610.
- (30) Imada, M.; Fujimori, A.; Tokura, Y. Metal-Insulator Transitions. *Rev. Mod. Phys.* **1998**, *70*, 1039–1263.
- (31) Wang, W. D.; He, D. W.; Xiao, W. S.; Wang, S. M.; Xu, J. A. Electrical Characterization in the Phase Transition between Cubic PbCrO<sub>3</sub> Perovskites at High Pressures. *Chin. Phys. Lett.* **2013**, *30*, 117201.
- (32) Castillo-Martínez, E.; Arévalo-López, A. M.; Ruiz-Bustos, R.; Alario-Franco, M. A. Increasing the Structural Complexity of Chromium(IV) Oxides by High-Pressure and High-Temperature Reactions of CrO<sub>2</sub>. *Inorg. Chem.* **2008**, *47*, 8526–8542.
- (33) Alonso, J. A.; García-Muñoz, J. L.; Fernández-Díaz, M. T.; Aranda, M. A. G.; Martínez-Lope, M. J.; Casais, M. T. Charge Disproportionation in RNiO<sub>3</sub> Perovskites: Simultaneous Metal-Insulator and Structural Transition in YNiO<sub>3</sub>. *Phys. Rev. Lett.* **1999**, *82*, 3871–3874.
- (34) Wadati, H.; Takizawa, M.; Tran, T. T.; Tanaka, K.; Mizokawa, T.; Fujimori, A.; Chikamatsu, A.; Kumigashira, H.; Oshima, M.; Ishiwata, S.; et al. Valence Changes Associated with the Metal-Insulator Transition in Bi<sub>1-x</sub>La<sub>x</sub>NiO<sub>3</sub>. *Phys. Rev. B* **2005**, *72*, 155103.
- (35) Azuma, M.; Carlsson, S.; Rodgers, J.; Tucker, M. G.; Tsujimoto, M.; Ishiwata, S.; Isoda, S.; Shimakawa, Y.; Takano, M.; Attfield, J. P. Pressure-Induced Intermetallic Valence Transition in BiNiO<sub>3</sub>. *J. Am. Chem. Soc.* **2007**, *129*, 14433–14436.
- (36) Mizumaki, M.; Ishimatsu, N.; Kawamura, N.; Azuma, M.; Shimakawa, Y.; Takano, M.; Uozumi, T. Direct Observation of the Pressure-Induced Charge Redistribution in BiNiO<sub>3</sub> by X-ray Absorption Spectroscopy. *Phys. Rev. B* **2009**, *80*, 233104.